HHS Public Access

Author manuscript

Biomaterials. Author manuscript; available in PMC 2018 June 12.

Published in final edited form as:

Biomaterials. 2015 August ; 59: 172–181. doi:10.1016/j.biomaterials.2015.04.003.

Paracrine co-delivery of TGF-β and IL-2 using CD4-targeted nanoparticles for induction and maintenance of regulatory T cells

Michael D. McHugh[a], **Jason Park**[a], **Ross Uhrich**[a], **Wenda Gao**[b], **David A. Horwitz**[c], and **Tarek M. Fahmy**[a,d,*]

[a]Department of Biomedical Engineering, Yale University, 55 Prospect Street, 415 Malone Engineering Center, New Haven, CT 06511, USA

[b]Transplant Research Center, Beth Israel Hospital, Harvard Medical School, 77 Avenue Louis Pasteur, Boston, MA 02115, USA

[c]Keck School of Medicine, University of Southern California, 2011 Zonal Ave, Los Angeles, CA 90089, USA

[d]Department of Immunobiology, Yale University, 55 Prospect Street, 415 Malone Engineering Center, New Haven, CT 06511, USA

Abstract

The cytokine milieu is critical for orchestration of lineage development towards effector T cell (Teff) or regulatory T cell (Treg) subsets implicated in the progression of cancer and autoimmune disease. Importantly, the fitness and survival of the Treg subset is dependent on the cytokines Interleukin-2 (IL-2) and transforming growth factor beta (TGF-β). The production of these cytokines is impaired in auto-immunity increasing the probability of Treg conversion to aggressive effector cells in a proinflammatory microenvironment. Therapy using soluble TGF-β and IL-2 administration is hindered by the cytokines' toxic pleiotropic effects and hence bioavailability to $CD4^+$ T cell targets. Thus, there is a clear need for a strategy that rectifies the cytokine milieu in autoimmunity and inflammation leading to enhanced Treg stability, frequency and number. Here we show that inert biodegradable nanoparticles (NP) loaded with TGF-β and IL-2 and targeted to $CD4^+$ cells can induce $CD4^+$ Tregs *in-vitro* and expand their number *in-vivo*. The stability of induced Tregs with cytokine-loaded NP was enhanced leading to retention of their suppressive phenotype even in the presence of proinflammatory cytokines. Our results highlight the importance of a nanocarrier-based approach for stabilizing and expanding Tregs essential for cell-immunotherapy of inflammation and autoimmune disease.

*Corresponding author. Department of Immunobiology, Yale University, 55 Prospect Street, 415 Malone Engineering Center, New Haven, CT 06511, USA.

M.D.M. designed research, performed experiments, analyzed data, and wrote paper. J.P. designed and performed experiments and analyzed data. R.U. performed experiments. W.G. supplied reagents. D.H. designed experiments. T.M.F. designed research and wrote paper.

Keywords

Autoimmunity; Drug delivery; Immunomodulation; Nanoparticles; TGF-β; Interleukin-2

1. Introduction

Tregs that express the Forkhead box protein transcription factor (Foxp3) are a critical subset of $CD4^+$ T cells that maintain homeostasis during infection and tolerance toward self-epitopes [1–3]. Mutations in Foxp3 can lead to the wasting multi-organ autoimmune condition, IPEX (immune-dysregulation, poly-endocrinopathy, enteropathy, X-linked) in humans [4]. In many common autoimmune diseases such as multiple sclerosis and type 1 diabetes [5,6], Tregs are unable to control pathogenic $CD4^+$ and $CD8^+$ effector cells because of defects related to their numbers or function [7–11]. For this reason, strategies to correct these defects and boost their stability have been garnering attention as potential alternatives to the conventional broadly immunosuppressive agents currently in use [12].

$Foxp3^+$ Tregs are now classified as one of three subsets [13]. The majority of endogenous Tregs are derived from the thymus and called natural Tregs (nTregs) [1]. These nTregs characteristically display chromatin demethylation at the Foxp3 locus [14,15]. Peripheral Tregs (pTregs) can also be peripherally differentiated from naïve T cells. Similarly, inducible Tregs (iTregs) can be generated from naïve $CD4^+$ cells *ex-vivo* by suboptimal TCR signaling in the presence of IL-2 and TGF-β [16–18]. Importantly, recent studies comparing the stability of mouse and human nTregs and iTregs in an inflammatory microenvironment have revealed that only iTregs remain $Foxp3^+$ and can reverse established disease [19–21]. These findings are supported by the recent report that Tregs induced *in-vivo* can also reverse disease in animal models of multiple sclerosis and autoimmune diabetes [22]. However, the methods used to induce these protective iTregs are translationally challenging because of the toxicity associated with delivery of pleiotropic cytokines. By designing a system able to safely provide TGF-β and IL-2 needed for stable Tregs [23,24], we aimed to generate a functionally robust inducible CD4 Treg population *in-vivo*.

Prior studies have utilized nanoparticles to deliver bioactive agents to modulate T cell activation through surface-binding [25–27], but use of these systems to support $Foxp3^+$ Treg function remains largely unexplored. Therefore, we chose to use nanoparticles composed of poly(lactic-co-glycolic) acid (PLGA), which have been used extensively for the controlled delivery of various proteins to many cell types [28–30]. Given the clear goal here, directed delivery of pleiotropic cytokines to $CD4^+$ T cells, and its clinical implication for autoimmune treatment, we chose to use the simplest and most ubiquitous nanocarrier delivery system. PLGA degradation and subsequent release of embedded agents is well understood. It is an FDA approved polymer that degrades via hydrolysis, and release of encapsulated proteins can be programmed over the course of several days to weeks depending on the composition of the polymer matrix [31]. For example, artificial antigen-presentation systems using PLGA particles loaded with IL-2 enhance CD8 T cell proliferation and function due to local accumulation of cytokines at the interface between particles and cells [32,33]. PLGA micro- and nanoparticles surface-conjugated with

antibodies have been shown to facilitate attachment to different specific cell types [26,34,35]. Given the platform's capacity to generate and maintain tunable cytokine conditions at a target cell surface, we therefore explored its potential for Treg induction by delivery of TGF-β and IL-2 to $CD4^+$ T cells. In this study, we characterized the CD4 cell-binding capacity of the particles and their ability to generate Tregs *in-vitro* and *in-vivo*. Furthermore we show that nanoparticle-induced Tregs are more efficacious in both their suppressive function and phenotypic stability in comparison to conventionally induced Tregs.

2. Materials and methods

2.1. Nanoparticle synthesis

Human recombinant TGF-β1 (mammalian-derived, Peprotech, Rocky Hill, NJ) and human recombinant IL-2 (Proleukin) was encapsulated in avidin-coated PLGA nanoparticles using a water/oil/water emulsion technique as previously described [36]. Briefly, 2.5 μg of aqueous cytokine solution was added drop-wise while vortexing to 50 mg PLGA (50:50 monomer ratio, Durect Corp) in 3 mls chloroform. The resulting emulsion was added dropwise to 3 mls of water containing 3% poly-vinyl alcohol (Sigma–Aldrich) and 0.625 mg/ml avidin–palmitate conjugate (previously described elsewhere [36]). This double emulsion was then sonicated to create nano-sized droplets of chloroform containing encapsulated cytokine, within aqueous surfactant. Solvent was removed by magnetic stirring at room temperature for 3 h. Hardened nanoparticles were then washed 3 times in MilliQ water and lyophilized for long-term storage. Nanoparticles were prepared fresh from lyophilized stocks for each experiment. Briefly, nanoparticles were dispersed in PBS at 10 mg/ml by vortexing and 2–3 s of bath sonication. CD4-targeted nanoparticles were formed by reacting avidin-coated nanoparticles in PBS with 2 μg biotin-anti-CD4 (RM 4-5, eBiosciences) per mg NP for 15 min and used immediately.

2.2. Characterization of nanoparticle size and morphology

Nanoparticle morphology was analyzed via scanning electron microscopy (SEM). Samples were sputter-coated with gold using a Dynavac Mini Coater and imaged with a Hitachi SU-70 SEM with an accelerating voltage of 5 kV. Particle size was quantified using the Nanosight particle tracking system (NanoSight, Ltd., Wiltshire, UK). Cytokine release was measured by incubating 1.0 mg nanoparticles in 1 ml PBS at 37 °C and measuring cytokine concentration in supernatant fractions over time by ELISA.

2.3. Imaging of T cell-NP interactions

10 μg of DiR-encapsulating nanoparticles conjugated to CD4 or isotype antibodies was added to C57BL/6 splenocytes (1.0×10^6/ml) and tumbled for 15 min at 37 °C in 1.5 ml microcentrifuge tubes. Cells were then stained for CD4-PE and analyzed using an Amnis Imagestream instrument.

2.4. Cell culture

All cell culture was performed at 37 °C, 5.0% CO_2, 100% humidity in RPMI-1640 (Life Technologies) supplemented with 10% FBS (Atlanta Biologics), Pen/Strep, L-glutamine,

MEM Vitamin solution, non-essential amino acids, sodium pyruvate, and beta-mercaptoethanol (Life Technologies).

2.5. Functional characterization of nano-encapsulated IL-2

CRL-1841 cells (ATCC, Manassas, VA) were seeded at 5.0×10^4 cells per well of a 96-well plate and dosed with free IL-2 or IL-2 encapsulated in untargeted nanoparticles. Fold proliferation was quantified by Coulter Counter after 4 days of culture.

2.6. Animals

C57BL/6 and BALB/c mice were purchased from Jackson Labs and Harlan, respectively, for use at 6–12 weeks of age. Mice expressing GFP as a reporter of Foxp3 expression (GFP-Foxp3 reporter mice) were generated on a C57BL/6 background as previously described [37]. All animal work was performed under protocols approved by the Yale Institute of Animal Care and Use Committee.

2.7. Staining, FACS, and cytokine secretion analysis

Cells were stained with CellTrace Violet (Life Technologies) following the manufacturers suggested protocol. After red blood cell lysis, splenocyte pellets were resuspended in 10 μM solution of CellTrace Violet in DPBS and incubated for 15 min at 37 °C. The reaction was then quenched using 5× volume of RPMI+10% FBS, and cells were pelleted once more to wash away free CellTrace Violet dye. For the Treg suppressor assay (Fig. 4), responder cells were labeled with CellTrace Violet after FACS purification and plated immediately.

Fluorescent antibodies were purchased from eBiosciences and used in dilutions of 1:200 or 1:400 in FACS buffer (PBS containing 2% FBS) for surface staining. CD4 was detected using clone RM 4-4 to avoid competitive binding with nanoparticle-conjugated RM 4-5. Cells were incubated with antibodies for 20–30 min and washed once in FACS buffer. For experiments requiring Foxp3 staining, samples were treated with 250 ul of Fix/Perm buffer (Intracellular Fixation and Permeabilization Kit, eBiosciences) after washing off surface antibodies. After 30–60 min, samples were washed with 2.0 mls Perm buffer and incubated with Foxp3 antibody (clone FJK-16s, eBioscience) for 30–60 min. Cells were then washed with 2.0 mls Perm buffer. After staining, cells were suspended in 1% PFA until FACS analysis up to 24 h later. All incubations in the immunostaining procedures were carried out in the dark on ice.

FACS analysis was performed on either a FACScan or LSR-II (Becton Dickinson), and sorting was done on a FACSAria (Becton Dickinson). All FACS data were analyzed using FlowJo software (Tree Star Inc., Ashland, OR).

TGF-β and IL-10 secretion was quantified by ELISA using kits purchased from Becton Dickinson, following the manufacturer's suggested instructions. Total TGF-β was measured by activating latent cytokine by incubating supernatants with 0.04 N HCl for 1 h and neutralizing with NaCl. TGF-β supplied by the treatment was subtracted from the measured values to quantify secretion.

2.8. In-vitro Treg induction and expansion

Freshly isolated mouse splenocytes were plated in 96-well round bottom plates at 1.0×10^5 cells in 0.2 ml per well. Wells were pre-coated with anti-CD3 (eBiosciences) at 2.0 μg/ml and media was supplemented with 2.0 μg/ml anti-CD28 (eBiosciences). For Treg induction conditions, media was supplemented with TGF-β and IL-2 at 5.0 ng/ml and 10 U/ml, respectively, unless otherwise stated. For kinetic analysis of Foxp3 expression, cells were removed from culture at day 3, washed twice in media to remove unbound nanoparticles and free cytokine, and re-seeded in fresh wells containing CD3 and CD28. For Foxp3 destabilizing conditions, TGF-β and IL-6 were added at re-seeding at 5.0 and 10 ng/ml, respectively. Nanoparticles were prepared as described above and added to cells at 100 μg/ml, unless otherwise stated.

2.9. Treg suppression assay

Tregs were generated from Foxp3-GFP reporter mouse (Thy1.1$^-$) splenocytes using either soluble TGF-β and IL-2 or nano-encapsulated TGF-β and IL-2 for a 5 day induction period beginning with 1×10^5 cells per well in 96-well U-bottom plates. At the end of culture, the percentage of CD4$^+$Foxp3$^+$ Tregs in each group was quantified by FACS. Cells were washed of excess nanoparticles or cytokines by centrifugation. These cells, defined collectively as the suppressor population, were mixed with FACS-purified, Cell-Trace Violet labeled Thy1.1$^+$ CD4$^+$CD25$^-$ splenocytes, (defined as responder cells) at titrated frequencies and stimulated with CD3/CD28 beads (Dynabeads, Life Technologies) at a 1:2 bead-to-cell ratio for 4 days in 96-well flat-bottom plates. Samples were surface stained for CD4 and Thy1.1 and run on FACS immediately.

Proliferative Index was calculated by dividing the total number of responder cells at the end of culture by the number of parent responder cells. Total number of cells was calculated by gating on each generation and accounting for number of divisions, using an area under the curve summation formula previously reported [38] and defined in Table 2. Initial Treg frequency, or the percentage of Thy1.1$^-$Foxp3$^+$ Tregs in culture at the start of the suppression phase is defined in Table 2.

2.10. In-vivo biodistribution and Treg quantification

6–8 week old female C57/Bl6 mice received coumarin-6 loaded nanoparticles via intraperitoneal injection on day 0. On day 5, mice were sacrificed and secondary lymphoid tissues were collected, including the spleen, axial lymph nodes (aLN), mesenteric lymph nodes (mLN), and inguinal lymph nodes (iLN). For analysis of coumarin-6 loaded nanoparticle biodistribution, whole spleen or lymph samples were homogenized and subjected to 3 freeze/thaw cycles prior to lyophilization. Coumarin 6 was extracted by incubation of homogenized tissues in DMSO and quantified using standards generated in tissues from untreated mice, by fluorescence with excitation/emission at 460/540 nm.

For Treg quantification, tissues were processed and stained for CD4, CD25, and Foxp3 as previously described and analyzed by FACS. Cells were counted using a Coulter Counter.

3. Results

3.1. Nanoparticle fabrication and characterization

PLGA nanoparticles encapsulating TGF-β and IL-2 were visualized using scanning electron microscopy (SEM, Fig. 1A). Nano-particles are spherical in morphology and range in size from less than 100 nm–300 nm. Quantitative size analysis was performed using the Nanosight® particle tracking system, which confirmed the size distribution and revealed a mean particle size of 168 nm (Fig. 1B). To measure the release kinetics of encapsulated cytokines over the course of nanoparticle degradation, we incubated the particles in PBS and performed ELISAs on their supernatants over time. The resulting plot indicates a burst release of TGF-β and IL-2 over the first 4 days, followed by linear release for the next 14 days (Fig. 1C). At day 5 of incubation, 0.8 ng and 0.5 ng of TGF-β and IL-2, respectively, are released from each mg of nanoparticles. To verify the binding capacity of anti-CD4-conjugated nanoparticles to CD4 T cells, we incubated 1,1′-Dioctadecyl-3,3,3′,3′-tetramethylindotricarbocyanine iodide, AAT Bioquest (DiR) labeled, anti-CD4-conjugated nanoparticles with mixed splenocytes. Following incubation, cells were stained for CD4-PE and analyzed using Amnis ImageStream Cytometry to visualize the particles' CD4 specificity and cellular localization. Targeting with anti-CD4 increases specific binding from 10.8% to 61.6%, while the percentage of $CD4^+$ cells tagged with nanoparticles is enhanced from 3.97% to 73.9% (Fig. 2A). Nanoparticles bind to the outer membrane of CD4 T cells (Fig. 2B). In all subsequent experiments, nanoparticles are coated with anti-CD4 unless otherwise stated.

3.2. Nano-encapsulated cytokines generate $Foxp3^+$ CD4 Tregs

Foxp3-GFP reporter mouse splenocytes were depleted of $CD4^+CD25^+Foxp3^+$ cells by FACS. Pre-and post-depletion FACS plots are shown on the left and right columns, respectively (Fig. 3A). Cells were stimulated with anti-CD3 and anti-CD28 in the presence of TGF-β and IL-2 for three days. $Foxp3^+$ $CD4^+$ cells are generated in both the nTreg depleted and non-depleted groups (18.9% and 21.9% of lymphocytes, respectively), indicating that TGF-β and IL-2 induce Foxp3 expression from naïve CD4 cells.

After 5 days of Treg induction by either nano-encapsulated or free TGF-β and IL-2, cells secreted TGF-β and IL-10 as measured by ELISA (Fig. 3B). Representative FACS plots show that Foxp3 expression is increased by nearly 2-fold using nano-encapsulated IL-2 and TGF-β compared to soluble cytokines (Fig. 3C). Cumulative data from four independent experiments shows significant differences between each group (Fig. 3D). Dose response curves show that lower concentrations of TGF-β released from 0.1 mg/ml targeted or untargeted nanoparticles is needed for Foxp3 expression compared to soluble TGF-β (Fig. 3E). IL-2 dependent cells require 10 fold less IL-2 released from nanoparticles in comparison with soluble IL-2 for equivalent proliferation (Fig. 3F).

3.3. Functional properties of nanoparticle-induced Tregs

To test suppressive function, induced Tregs were washed and cultured under CD3/CD28 stimulation with responder $Thy1.1^+$ CD4 cells at various relative fractions of Tregs over a four-day period referred to as the suppression phase. For clarity, we refer to each cell

population using a superscript/subscript notation defined in Table 1. Characterization terms are defined in Table 2. A schematic of the experimental procedure as a representative cell response over time is shown (Fig. 4A). At the end of the suppression phase, the resulting CD4 pool was characterized by plotting Thy1.1 expression vs. Cell-Trace Violet incorporation as shown in a representative FACS plot (Fig. 4B). Suppressor cells $f_{1.1-}^{CD4}$ ere identified by absence of Cell-Trace Violet and Thy1.1 expression, and Responder cells $f_{1.1+}^{CD4}$ were identified as Thy1.1^{+} CellTrace Violet intermediate-to-high, representing proliferated and undivided cells, respectively. Responder cells were plotted on a histogram according to CellTrace Violet incorporation and gated for generation number as shown in a representative histogram (Fig. 4C). Representative histograms from each initial Treg fraction from each group show reduced CellTrace Violet dilutions in nanoparticle-treated groups (Fig. 4D). Proliferative Indices calculated from the above data are graphed, revealing significantly lower responder cell proliferation in nanoparticle groups at all initial Treg fractions tested (Fig. 4E).

Nanoparticle-treated suppressor cells also retained Foxp3 expression to a greater extent to those induced using soluble cytokines. Representative FACS plots from each group are shown (Fig. 4F). Foxp3 quantifications are plotted over initial Treg fraction, showing that greatest relative Foxp3 expression is found at 1/2 initial Treg fractions, approximately 3-fold higher than soluble controls (Fig. 4G). Absolute number of Foxp3^{+} Tregs within the suppressor population is calculated as described in Table 2 and plotted separately (Fig. 4H). The trend is retained, in which higher initial Treg fraction correlates with Foxp3 expression in the nanoparticle groups more closely than in soluble groups.

3.4. Foxp3 stability of nanoparticle-induced Tregs

In-vitro kinetics assays were performed to test the phenotype stability of nanoparticle-induced Tregs. Mixed splenocyte cultures were incubated with free or CD4-targeted nano-encapsulated cytokine before replacement with fresh media after 3 days. As a positive control, free cytokines were replenished at day 3. By day 9 of culture, Foxp3 expression by soluble cytokine-induced cells was nearly completely lost (98% less than day 5), while Foxp3 expressing nanoparticle-induced Tregs diminished by only 34% from day 5 (Fig. 5A). To evaluate Foxp3 stability under inflammatory insult, the Th17-polarizing cytokine combination TGF-β/IL-6 was added to the cultures after a 5-day Treg induction phase. At day 7, the number of CD25^{+}Foxp3^{+} CD4 cells was largely retained in the nanoparticle-induced cells (Fig. 5B).

3.5. Expansion of Tregs in-vivo

We next investigated the effects of nanoparticle-mediated cytokine delivery *in-vivo*. The biodistribution of CD4-targeted nanoparticles was investigated using coumarin 6 (C6)-loaded nanoparticles. Mice received a dose of 2.0 mgs of nanoparticles administered via intraperitoneal injection. After 5 days, animals were sacrificed and secondary lymphoid organs were collected for analysis. Extraction of C6 from the tissues showed the highest accumulation in the spleen and draining (mesenteric) lymph nodes (Fig. 6A). To assess the ability of nanoparticles to expand Tregs *in-vivo*, mice were injected with 2.0 mg CD4-

targeted nanoparticles. After 5 days, lymph nodes were collected and Treg induction was assessed by FACS. In comparison to naïve animals (black), nanoparticle-treated animals (pink) had a significantly higher frequency of Tregs in the mesenteric lymph node and spleen as measured by their frequency within the CD4 T cell compartment (Fig. 6B) (n = 5 mice, *p < 0.05). Total numbers of Tregs were not significantly enhanced (Fig. 6C). Representative FACS plots are gated on $CD4^+$ lymphocytes and identify $CD25^+Foxp3^+$ Tregs for each tissue analyzed (Fig. 6D). Values on the lower left of the gate show Tregs as a percentage of $CD4^+$ cells and represent data in Fig. 6B, whereas values to the right show Tregs as a percentage of all lymphocytes, used to calculate absolute numbers plotted in Fig. 6C.

4. Discussion

Cytokine and cell-based immunotherapies have promising therapeutic in the treatment of both pathologic tolerance and immunity, but there are significant obstacles to overcome. $Foxp3^+$ Tregs in clinical trials for certain chronic immune-mediated inflammatory diseases [39,40] must be expanded from very small numbers. Because of their rapid turnover, they will need help for long-term maintenance *in-vivo*. Moreover, these Tregs can become unstable and even autoaggressive in the inflammatory environment characteristic of these diseases [41].

Low-dose recombinant IL-2 can reverse type 1 diabetes in NOD mice [42] and has achieved clinical benefit in a small number of patients with graft-versus-host disease or vasculitis [43,44]. However, IL-2 has a short half-life in circulation, requiring frequent doses to maintain its affect while minimizing off-target signaling [45].

In this manuscript, we have shown that directed delivery of the cytokines TGF-b and IL-2 via nanocarriers can enhance the generation of stable, functional Tregs. This strategy therefore offers a new approach to directly improve the efficacy of clinically-relevant cell-based therapies. Nanoparticles loaded with an optimized ratio (1:2) of IL-2:TGF-β targeted to CD4 cells signal cooperatively at the cell surface. TGF-β, a regulatory cytokine widely recognized as a Treg inducer, is commonly used in conjunction with IL-2 to generate CD4 Tregs *in-vitro* [46–48]. The efficiency of Treg induction after incubation with TGF-β and IL-2 was maintained after prior depletion of nTregs, showing that the cytokine combination can induce the differentiation of naïve $Foxp3^-$ CD4 T cells. Sustained release of both cytokines was comparable due to physiochemical similarities between both proteins. Both cytokines have individually been encapsulated in PLGA matrices previously [30,32], but they have not been co-encapsulated in the same particle. To verify preservation of each cytokine's structure following PLGA encapsulation and particle synthesis, we assayed for bioactivity during particle-mediated release. Interestingly, encapsulated cytokines displayed greater bioactivity compared to soluble counterparts. Enhanced bioactivity may be due to increased local concentration gradients, and this has been previously observed with encapsulated IL-2 [32]. Strikingly, with encapsulated TGF-β, not only was the signaling threshold reduced, but the Foxp3 induction plateau was increased, highlighting the impact of high local concentration gradients. Thus, the nanoparticle-mediated paracrine-delivery of IL-2 and TGF-β may be more effective at driving naïve CD4 cells to become Tregs.

Although this phenomenon has yet to be investigated, mathematical modeling of paracrine signaling reveals that diffusive cytokine transfer may trigger unexpected signaling outcomes through reorganization of membrane receptors [49]. TGF-β signaling requires surface dimerization of two receptor subunits [50–52], which may partially depend on this paracrine affect, leading to the observed enhancement by nanoparticle-mediated delivery.

In addition to more efficient generation of $Foxp3^+$ Tregs, we demonstrate here that nanoparticles induce Tregs that are more effective suppressors on a per cell basis. When $Foxp3^+$ Treg cell numbers were matched between soluble cytokine-induced suppressors and nanoparticle-generated suppressors, nanoparticle-induced suppressors showed superior ability to inhibit CD4 effector proliferation in response to TCR ligation and co-stimulation. This effect was retained down to 1/32 initial Treg fraction, and verified that nanoparticle binding to the Treg cell surface had no detrimental impact on their functional capacity, but facilitated enhanced function. In these experiments, nanoparticle-induced suppressor cells retained Foxp3 expression to a greater extent than soluble cytokine-induced suppressor cells, which showed no correlation between initial Treg fraction and final Foxp3 expression. This observation supports the hypothesis that nanoparticle-mediated delivery of TGF-β and IL-2 markedly reduces the loss of Foxp3 expression over time.

Results of our Foxp3 kinetic assays suggest that nanoparticle-mediated delivery of TGF-β and IL-2 may also help overcome T cell plasticity in the context of inflammation and typically observed with Treg cell therapy. Although adoptive transfer of ex-vivo induced Tregs are effective at treating diabetes in NOD mice, a growing body of work suggests that some of these cells can turn off Foxp3 expression and even revert to an effector phenotype within inflammatory environments [53,54]. Nanoparticle delivery can maintain local cytokine availability to targeted cells even within polarizing microenvironments, which is useful for maintenance of Foxp3 expression in the absence of endogenous regulatory factors. IP administration of nanoparticles can lead to accumulation in secondary lymphoid tissues such as the spleen, facilitating a localized cytokine milieu critical for T cell differentiation [55–57]. Here, systemic administration of CD4-targeted TGF-β+IL-2 nanoparticles significantly enhanced Treg frequency in these tissues as a percentage of CD4 cells. However, statistical significance was not achieved when measuring the absolute number of Tregs. This suggests the possibility of off-target cytokine effects, but the increase of Foxp3+ cells of the CD4 compartment is nonetheless functionally relevant. The lesser efficacy *in-vivo* in comparison to *in-vitro* was likely due to nonspecific uptake by phagocytic cells in these tissues [57], decreasing the availability of encapsulated cytokines for developing T cells. Particles engineered to minimize phagocytic uptake is a possible venue for future studies. Alternatively, particles directed to dendritic cells and loaded with tolerogenic peptides or tolerogenic agents can facilitate expansion of Tregs. Recent work has demonstrated the promise of this approach [58]. Ultimately a combination of both strategies maybe an optimal solution to the challenging problem of induction and expansion of therapeutic autoantigen-specific Tregs *in-vivo*.

5. Conclusions

By efficiently delivering both TGF-β and IL-2 to CD4 T cells, this platform circumvents several fundamental drawbacks of today's leading autoimmune therapies. Paracrine cytokine delivery significantly increased Treg induction, enhanced suppressive function, and Foxp3 expression was stable even in depolarizing conditions. Future studies will establish the optimal composition of loaded cytokines, frequency of injections, and possible synergistic effects with other targeted nanoparticles in a strategy to induce remission of various autoimmune diseases.

Acknowledgments

We thank Kevan Herold and Richard Flavell for intellectual input. This work was also supported in part by NIH Autoimmunity Center of Excellent Pilot Award U19 AI056363. It was also supported in part by a Pfizer Grant to T.M.F. We thank Dr. Micah Benson, John Douhan and Dr. Karim Dabbagh for intellectual input and discussion regarding this study.

Abbreviations

CD	cluster of differentiation
DMSO	dimethylsulfoxide
ELISA	enzyme-linked immunosorbent assay
FACS	fluorescent activated cell sorting
FBS	fetal bovine serum
GFP	green fluorescent protein
HCl	hydrochloric acid
mTOR	mammalian target of rapamycin
NaCl	sodium chloride
PE	phycoerythrin
PFA	paraformaldehyde
TCR	T cell receptor

References

1. Sakaguchi S, Yamaguchi T, Nomura T, Ono M. Regulatory T cells and immune tolerance. Cell. 2008; 133(5):775–87. [PubMed: 18510923]
2. Chaudhry A, Rudensky AY. Control of inflammation by integration of environmental cues by regulatory T cells. J Clin Invest. 2013; 123(3):939–44. [PubMed: 23454755]
3. Maloy KJ, Powrie F. Regulatory T cells in the control of immune pathology. Nat Immunol. 2001; 2(9):816–22. [PubMed: 11526392]
4. Wildin RS, Ramsdell F, Peake J, Faravelli F, Casanova JL, Buist N, et al. X-linked neonatal diabetes mellitus, enteropathy and endocrinopathy syndrome is the human equivalent of mouse scurfy. Nat Genet. 2001; 27(1):18–20. [PubMed: 11137992]

5. Roep BO, Peakman M. Antigen targets of type 1 diabetes autoimmunity. Cold Spring Harb Perspect Med. 2012; 2(4):a007781. [PubMed: 22474615]
6. Jager A, Dardalhon V, Sobel RA, Bettelli E, Kuchroo VK. Th1, Th17, and Th9 effector cells induce experimental autoimmune encephalomyelitis with different pathological phenotypes. J Immunol. 2009; 183(11):7169–77. [PubMed: 19890056]
7. Cao D, Malmstrom V, Baecher-Allan C, Hafler D, Klareskog L, Trollmo C. Isolation and functional characterization of regulatory CD25brightCD4+ T cells from the target organ of patients with rheumatoid arthritis. Eur J Immunol. 2003; 33(1):215–23. [PubMed: 12594850]
8. Viglietta V, Baecher-Allan C, Weiner HL, Hafler DA. Loss of functional suppression by CD4+CD25+ regulatory T cells in patients with multiple sclerosis. J Exp Med. 2004; 199(7):971–9. [PubMed: 15067033]
9. Sugiyama H, Gyulai R, Toichi E, Garaczi E, Shimada S, Stevens SR, et al. Dysfunctional blood and target tissue CD4+CD25high regulatory T cells in psoriasis: mechanism underlying unrestrained pathogenic effector T cell proliferation. J Immunol. 2005; 174(1):164–73. [PubMed: 15611238]
10. Lindley S, Dayan CM, Bishop A, Roep BO, Peakman M, Tree TI. Defective suppressor function in CD4(+)CD25(+) T-cells from patients with type 1 diabetes. Diabetes. 2005; 54(1):92–9. [PubMed: 15616015]
11. Balandina A, Saoudi A, Dartevelle P, Berrih-Aknin S. Analysis of CD4+CD25+ cell population in the thymus from myasthenia gravis patients. Ann N Y Acad Sci. 2003; 998:275–7. [PubMed: 14592885]
12. Zhou X, Kong N, Zou H, Brand D, Li X, Liu Z, et al. Therapeutic potential of TGF-beta-induced CD4(+) Foxp3(+) regulatory T cells in autoimmune diseases. Autoimmunity. 2011; 44(1):43–50. [PubMed: 20670119]
13. Abbas AK, Benoist C, Bluestone JA, Campbell DJ, Ghosh S, Hori S, et al. Regulatory T cells: recommendations to simplify the nomenclature. Nat Immunol. 2013; 14(4):307–8. [PubMed: 23507634]
14. Sakaguchi S, Sakaguchi N, Shimizu J, Yamazaki S, Sakihama T, Itoh M, et al. Immunologic tolerance maintained by CD25+ CD4+ regulatory T cells: their common role in controlling autoimmunity, tumor immunity, and transplantation tolerance. Immunol Rev. 2001; 182:18–32. [PubMed: 11722621]
15. Floess S, Freyer J, Siewert C, Baron U, Olek S, Polansky J, et al. Epigenetic control of the foxp3 locus in regulatory T cells. PLoS Biol. 2007; 5(2):e38. [PubMed: 17298177]
16. Chen Y, Kuchroo VK, Inobe J, Hafler DA, Weiner HL. Regulatory T cell clones induced by oral tolerance: suppression of autoimmune encephalomyelitis. Science. 1994; 265(5176):1237–40. [PubMed: 7520605]
17. Nakamura K, Kitani A, Strober W. Cell contact-dependent immunosuppression by CD4(+)CD25(+) regulatory T cells is mediated by cell surface-bound transforming growth factor beta. J Exp Med. 2001; 194(5):629–44. [PubMed: 11535631]
18. Kingsley CI, Karim M, Bushell AR, Wood KJ. CD25+CD4+ regulatory T cells prevent graft rejection: CTLA-4- and IL-10-dependent immunoregulation of alloresponses. J Immunol. 2002; 168(3):1080–6. [PubMed: 11801641]
19. Lu L, Wang J, Zhang F, Chai Y, Brand D, Wang X, et al. Role of SMAD and non-SMAD signals in the development of Th17 and regulatory T cells. J Immunol. 2010; 184(8):4295–306. [PubMed: 20304828]
20. Zheng SG, Wang J, Horwitz DA. Cutting edge: foxp3+CD4+CD25+ regulatory T cells induced by IL-2 and TGF-beta are resistant to Th17 conversion by IL-6. J Immunol. 2008; 180(11):7112–6. [PubMed: 18490709]
21. Kong N, Lan Q, Chen M, Wang J, Shi W, Horwitz DA, et al. Antigen-specific transforming growth factor beta-induced Treg cells, but not natural Treg cells, ameliorate autoimmune arthritis in mice by shifting the Th17/Treg cell balance from Th17 predominance to Treg cell predominance. Arthritis Rheum. 2012; 64(8):2548–58. [PubMed: 22605463]
22. Kasagi S, Zhang P, Che L, Abbatiello B, Maruyama T, Nakatsukasa H, et al. In vivo-generated antigen-specific regulatory T cells treat autoimmunity without compromising antibacterial immune response. Sci Transl Med. 2014; 6(241):241ra78.

23. Fontenot JD, Rasmussen JP, Gavin MA, Rudensky AY. A function for interleukin 2 in Foxp3-expressing regulatory T cells. Nat Immunol. 2005; 6(11):1142–51. [PubMed: 16227984]
24. Li MO, Wan YY, Flavell RA. T cell-produced transforming growth factor-beta1 controls T cell tolerance and regulates Th1- and Th17-cell differentiation. Immunity. 2007; 26(5):579–91. [PubMed: 17481928]
25. Fahmy TM, Schneck JP, Saltzman WM. A nanoscopic multivalent antigen-presenting carrier for sensitive detection and drug delivery to T cells. Nanomed Nanotechnol Biol Med. 2007; 3(1):75–85.
26. Park J, Gao W, Whiston R, Strom TB, Metcalfe S, Fahmy TM. Modulation of CD4+ T lymphocyte lineage outcomes with targeted, nanoparticle-mediated cytokine delivery. Mol Pharm. 2011; 8(1): 143–52. [PubMed: 20977190]
27. Stephan MT, Moon JJ, Um SH, Bershteyn A, Irvine DJ. Therapeutic cell engineering with surface-conjugated synthetic nanoparticles. Nat Med. 2010; 16(9):1035–41. [PubMed: 20711198]
28. Mundargi RC, Babu VR, Rangaswamy V, Patel P, Aminabhavi TM. Nano/micro technologies for delivering macromolecular therapeutics using poly(D,L-lactide-co-glycolide) and its derivatives. J Control Release: Off J Control Release Soc. 2008; 125(3):193–209.
29. Demento SL, Cui W, Criscione JM, Stern E, Tulipan J, Kaech SM, et al. Role of sustained antigen release from nanoparticle vaccines in shaping the T cell memory phenotype. Biomaterials. 2012; 33(19):4957–64. [PubMed: 22484047]
30. Jhunjhunwala S, Balmert SC, Raimondi G, Dons E, Nichols EE, Thomson AW, et al. Controlled release formulations of IL-2, TGF-beta1 and rapamycin for the induction of regulatory T cells. J Control Release: Off J Control Release Soc. 2012; 159(1):78–84.
31. Mahapatro A, Singh DK. Biodegradable nanoparticles are excellent vehicle for site directed in-vivo delivery of drugs and vaccines. J Nanobiotechnol. 2011; 9:55.
32. Steenblock ER, Fadel T, Labowsky M, Pober JS, Fahmy TM. An artificial antigen-presenting cell with paracrine delivery of IL-2 impacts the magnitude and direction of the T cell response. J Biol Chem. 2011; 286(40):34883–92. [PubMed: 21849500]
33. Steenblock ER, Fahmy TM. A comprehensive platform for ex vivo T-cell expansion based on biodegradable polymeric artificial antigen-presenting cells. Mol Ther: J Am Soc Gene Ther. 2008; 16(4):765–72.
34. Keegan ME, Royce SM, Fahmy T, Saltzman WM. In vitro evaluation of biodegradable microspheres with surface-bound ligands. J Control Release: Off J Control Release Soc. 2006; 110(3):574–80.
35. Park J, Mattessich T, Jay SM, Agawu A, Saltzman WM, Fahmy TM. Enhancement of surface ligand display on PLGA nanoparticles with amphiphilic ligand conjugates. J Control Release: Off J Control Release Soc. 2011; 156(1):109–15.
36. Fahmy TM, Samstein RM, Harness CC, Mark Saltzman W. Surface modification of biodegradable polyesters with fatty acid conjugates for improved drug targeting. Biomaterials. 2005; 26(28): 5727–36. [PubMed: 15878378]
37. Bettelli E, Carrier Y, Gao W, Korn T, Strom TB, Oukka M, et al. Reciprocal developmental pathways for the generation of pathogenic effector TH17 and regulatory T cells. Nature. 2006; 441(7090):235–8. [PubMed: 16648838]
38. Roederer M. Interpretation of cellular proliferation data: avoid the panglossian. Cytometry Part A: J Int Soc Anal Cytol. 2011; 79(2):95–101.
39. Brunstein CG, Miller JS, Cao Q, McKenna DH, Hippen KL, Curtsinger J, et al. Infusion of ex vivo expanded T regulatory cells in adults transplanted with umbilical cord blood: safety profile and detection kinetics. Blood. 2011; 117(3):1061–70. [PubMed: 20952687]
40. Marek-Trzonkowska N, Mysliwiec M, Dobyszuk A, Grabowska M, Derkowska I, Juscinska J, et al. Therapy of type 1 diabetes with CD4(+) CD25(high)CD127-regulatory T cells prolongs survival of pancreatic islets – results of one year follow-up. Clin Immunol. 2014; 153(1):23–30. [PubMed: 24704576]
41. Riley JL, June CH, Blazar BR. Human T regulatory cell therapy: take a billion or so and call me in the morning. Immunity. 2009; 30(5):656–65. [PubMed: 19464988]

42. Grinberg-Bleyer Y, Baeyens A, You S, Elhage R, Fourcade G, Gregoire S, et al. IL-2 reverses established type 1 diabetes in NOD mice by a local effect on pancreatic regulatory T cells. J Exp Med. 2010; 207(9):1871–8. [PubMed: 20679400]
43. Koreth J, Matsuoka K, Kim HT, McDonough SM, Bindra B, Alyea EP 3rd, et al. Interleukin-2 and regulatory T cells in graft-versus-host disease. N Engl J Med. 2011; 365(22):2055–66. [PubMed: 22129252]
44. Saadoun D, Rosenzwajg M, Joly F, Six A, Carrat F, Thibault V, et al. Regulatory T-cell responses to low-dose interleukin-2 in HCV-induced vasculitis. N Engl J Med. 2011; 365(22):2067–77. [PubMed: 22129253]
45. Long SA, Buckner JH, Greenbaum CJ. IL-2 therapy in type 1 diabetes: “Trials” tribulations. Clin Immunol. 2013; 149(3):324–31. [PubMed: 23499139]
46. Fantini MC, Becker C, Tubbe I, Nikolaev A, Lehr HA, Galle P, et al. Transforming growth factor beta induced FoxP3+ regulatory T cells suppress Th1 mediated experimental colitis. Gut. 2006; 55(5):671–80. [PubMed: 16162681]
47. Chen W, Jin W, Hardegen N, Lei KJ, Li L, Marinos N, et al. Conversion of peripheral CD4+CD25- naive T cells to CD4+CD25+ regulatory T cells by TGF-beta induction of transcription factor Foxp3. J Exp Med. 2003; 198(12):1875–86. [PubMed: 14676299]
48. Fantini MC, Dominitzki S, Rizzo A, Neurath MF, Becker C. In vitro generation of CD4+ CD25+ regulatory cells from murine naive T cells. Nat Protoc. 2007; 2(7):1789–94. [PubMed: 17641646]
49. Labowsky M, Fahmy TM. Diffusive transfer between two intensely interacting cells with limited surface kinetics. Chem Eng Sci. 2012; 74:114–23. [PubMed: 22485051]
50. Wrana JL, Attisano L, Wieser R, Ventura F, Massague J. Mechanism of activation of the TGF-beta receptor. Nature. 1994; 370(6488):341–7. [PubMed: 8047140]
51. Moustakas A, Lin HY, Henis YI, Plamondon J, O’Connor-McCourt MD, Lodish HF. The transforming growth factor beta receptors types I, II, and III form hetero-oligomeric complexes in the presence of ligand. J Biol Chem. 1993; 268(30):22215–8. [PubMed: 7693660]
52. Letourneur O, Goetschy JF, Horisberger M, Grutter MG. Ligand-induced dimerization of the extracellular domain of the TGF-beta receptor type II. Biochem Biophys Res Commun. 1996; 224(3):709–16. [PubMed: 8713111]
53. Komatsu N, Mariotti-Ferrandiz ME, Wang Y, Malissen B, Waldmann H, Hori S. Heterogeneity of natural Foxp3+ T cells: a committed regulatory T-cell lineage and an uncommitted minor population retaining plasticity. Proc Natl Acad Sci U S A. 2009; 106(6):1903–8. [PubMed: 19174509]
54. Zhou X, Bailey-Bucktrout SL, Jeker LT, Penaranda C, Martinez-Llordella M, Ashby M, et al. Instability of the transcription factor Foxp3 leads to the generation of pathogenic memory T cells in vivo. Nat Immunol. 2009; 10(9):1000–7. [PubMed: 19633673]
55. Maincent P, Thouvenot P, Amicabile C, Hoffman M, Kreuter J, Couvreur P, et al. Lymphatic targeting of polymeric nanoparticles after intraperitoneal administration in rats. Pharm Res. 1992; 9(12):1534–9. [PubMed: 1488394]
56. Shirali AC, Look M, Du W, Kassis E, Stout-Delgado HW, Fahmy TM, et al. Nanoparticle delivery of mycophenolic acid upregulates PD-L1 on dendritic cells to prolong murine allograft survival. Am J Transpl: Off J Am Soc Transpl Am Soc Transpl Surg. 2011; 11(12):2582–92.
57. Look M, Stern E, Wang QA, DiPlacido LD, Kashgarian M, Craft J, et al. Nanogel-based delivery of mycophenolic acid ameliorates systemic lupus erythematosus in mice. J Clin Invest. 2013; 123(4):1741–9. [PubMed: 23454752]
58. Maldonado RA, LaMothe RA, Ferrari JD, Zhang AH, Rossi RJ, Kolte PN, et al. Polymeric synthetic nanoparticles for the induction of antigen-specific immunological tolerance. Proc Natl Acad Sci U S A. 2015; 112(2):E156–65. [PubMed: 25548186]

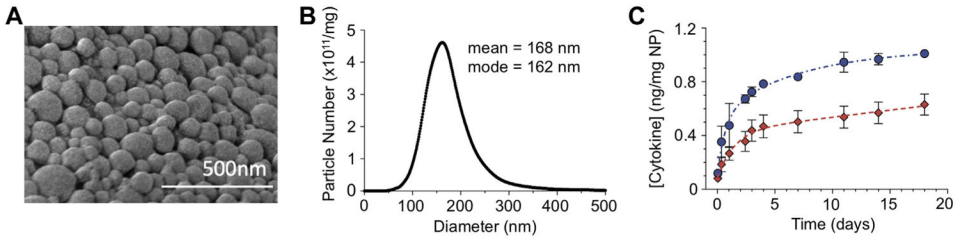

Fig. 1.

Characterization of PLGA nanoparticles containing TGF-β and IL-2 (A) Scanning electron microscopy of TGF-β+IL-2 nanoparticles. (B) Quantification of nanoparticle size distribution by Nanosight particle tracking system. (C) Release kinetics of TGF-β (blue circles) and IL-2 (red diamonds), measured by ELISA. (For interpretation of the references to colour in this figure legend, the reader is referred to the web version of this article.)

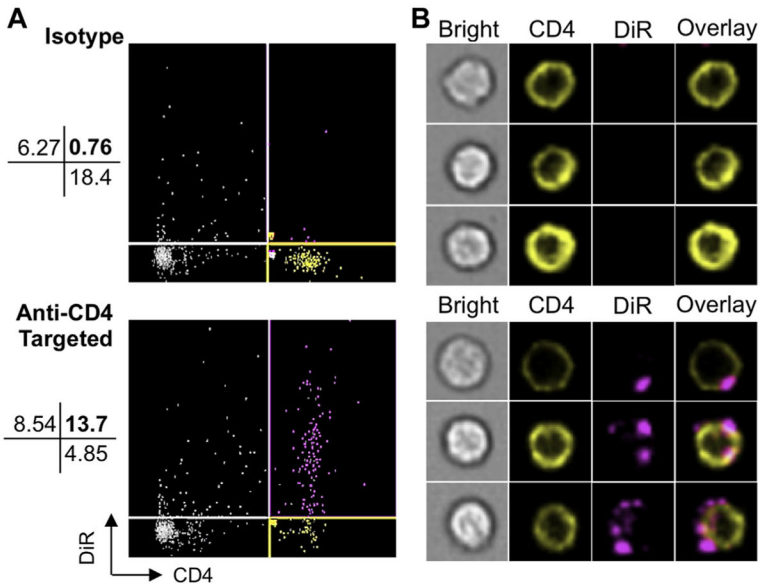

Fig. 2.

Targeted nanoparticles bind CD4 cells. (A) After incubating 10 μg DiR-labeled nanoparticles with 1 × 106 mouse splenocytes for 20 min at 37 °C, FACS plots were generated using Amnis Imagestream. (B) Fluorescent imaging illustrates targeting-dependent surface-binding of nanoparticles to $CD4^+$ cells.

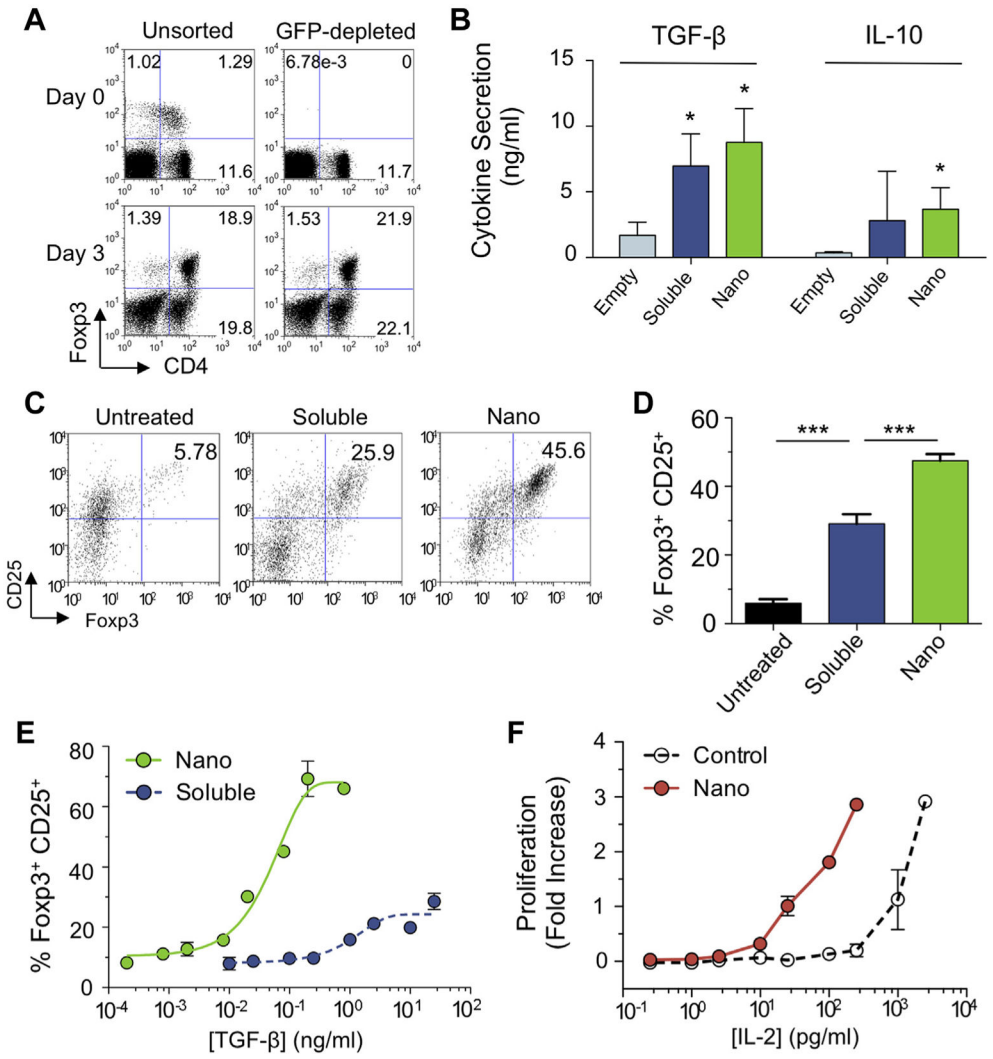

Fig. 3.

Nano-encapsulated cytokines generate Foxp3$^+$ CD4 Tregs. (A) Naïve or nTreg-depleted splenocytes were incubated with 5 ng/ml TGF-β and 50 U/ml IL-2 for 4 days and resulting Treg induction was analyzed by FACS. (B) In a separate experiment, mixed splenocytes were cultured with TGF-β and IL-2 in soluble (5 ng/ml and 10 U/ml, respectively) or nano-encapsulated form (0.1 mg nanoparticle/ml) to induce CD25$^+$Foxp3$^+$ Tregs. TGF-β and IL-10 concentrations in the supernatant were measure by ELISA. (C) Representative FACS plots showing Foxp3 induction are gated on CD4$^+$ lymphocytes. (D) Results from 4 independent experiments are plotted (***P < 0.001). (E) Dose responses of nano-encapsulated (green), and soluble (blue) cytokine. Values are percentages of CD4$^+$ lymphocytes. (F) IL-2 dependent CTRL-1842 cells were dosed with nano-encapsulated vs. free IL-2 and proliferation was quantified after 4 days by Coulter Counter. (For interpretation of the references to colour in this figure legend, the reader is referred to the web version of this article.)

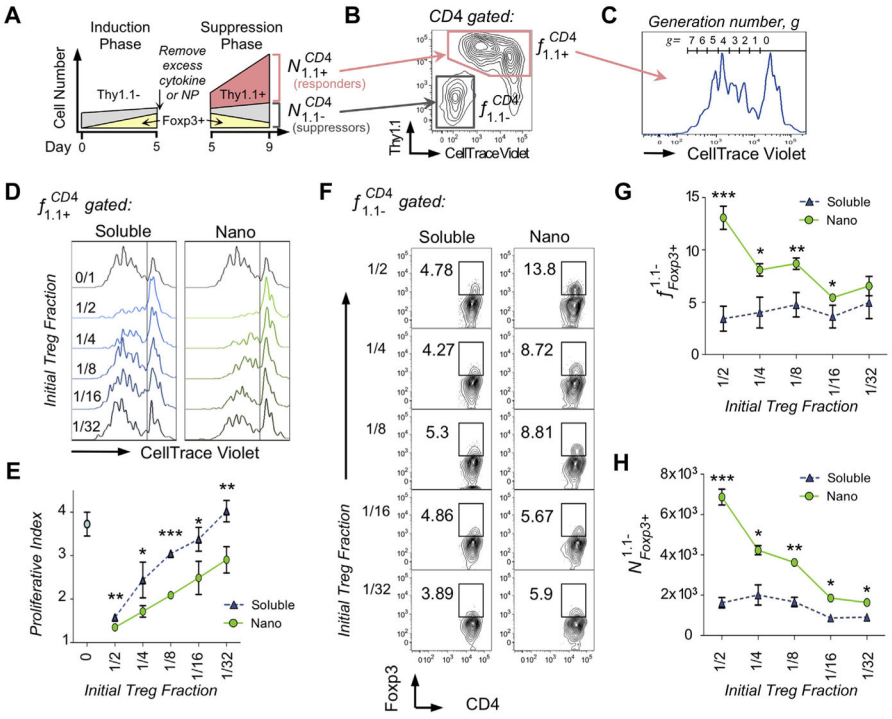

Fig. 4.

Nanoparticle-induced Tregs have enhanced suppressive function. (A) A schematic of the experimental setup shows representative cell numbers over time. Suppressor cells (Thy1.1^{-}) were generated by activating T cells with plate bound anti-CD3 and soluble anti-CD28 with either free IL-2 and TGF-β (10 U/ml and 5 ng/ml, respectively), or nanoparticles (0.1 mg/ml) for 5 days (induction phase). Foxp3^{+} Tregs (yellow) were quantified by FACS, washed, and added in various relative Treg fractions to CD4^{+}Thy1.1^{+}CD25^{-} splenocytes (responder cells, pink). These cultures were stimulated with anti-CD3/CD28 beads in 96-well flat-bottom plates at a 1:2 bead-to-cell ratio for an additional 4 days (suppression phase). During this period, responder cells proliferated while Foxp3 expression on suppressor cells decreased. (B) Following the suppression phase, suppressor and responder cells were identified by surface expression of Thy1.1 and incorporation of CellTrace Violet as shown in the representative FACS plot. (C) Each generation of proliferated responder cells was gated as shown in the representative histogram, and gated frequencies were used to calculate proliferative index, *PI*, as described in Table 2. (D) Representative CellTrace Violet dilutions across titrated initial Treg fractions shows that suppressor cells treated with nanoparticles preferentially suppressed responder proliferation. (E) Proliferative index of responder cells co-cultured with suppressor cells generated with soluble cytokines (blue triangles) vs. nano-encapsulated cytokines (green circles) is plotted (*$p < 0.05$, **$p < 0.005$, ***$p < 0.001$). (F) Representative FACS plots compare Foxp3 expression of suppressor cells at the end of the 4-day suppression period, showing elevated Foxp3 expression in the nano-encapsulated group. (G) Foxp3 expression of suppressor cells is plotted as a function of initial Treg fraction. (H) Total numbers of remaining Foxp3^{+} suppressor cell numbers are plotted as a function of initial Treg fraction. (*$p < 0.05$, **$p < 0.005$, ***$p < 0.001$). (For

interpretation of the references to colour in this figure legend, the reader is referred to the web version of this article.)

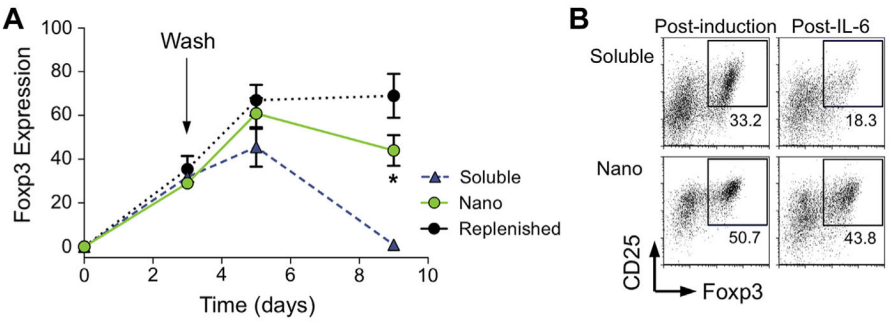

Fig. 5.

Nano-encapsulated cytokines enhance Treg stability. (A) Mixed splenocytes were treated with soluble (blue triangles) or nano-encapsulated (green circles) TGF-β and IL-2 for a 3 day induction phased before washing the cells and replating, and Foxp3 expression was monitored over time. Control cells (black circles) were replenished with soluble cytokine after washing. (*$p < 0.05$ between nano-encapsulated and soluble using a 2-tailed T test on day 9 Foxp3 expression). (B) After a 5 day induction phase, cells were washed and reseeded in the presence of TGF-β (5 nm/ml) and IL-6 (10 ng/ml) for Th17 polarization. FACS plots show CD4 phenotype at day 7. (For interpretation of the references to colour in this figure legend, the reader is referred to the web version of this article.)

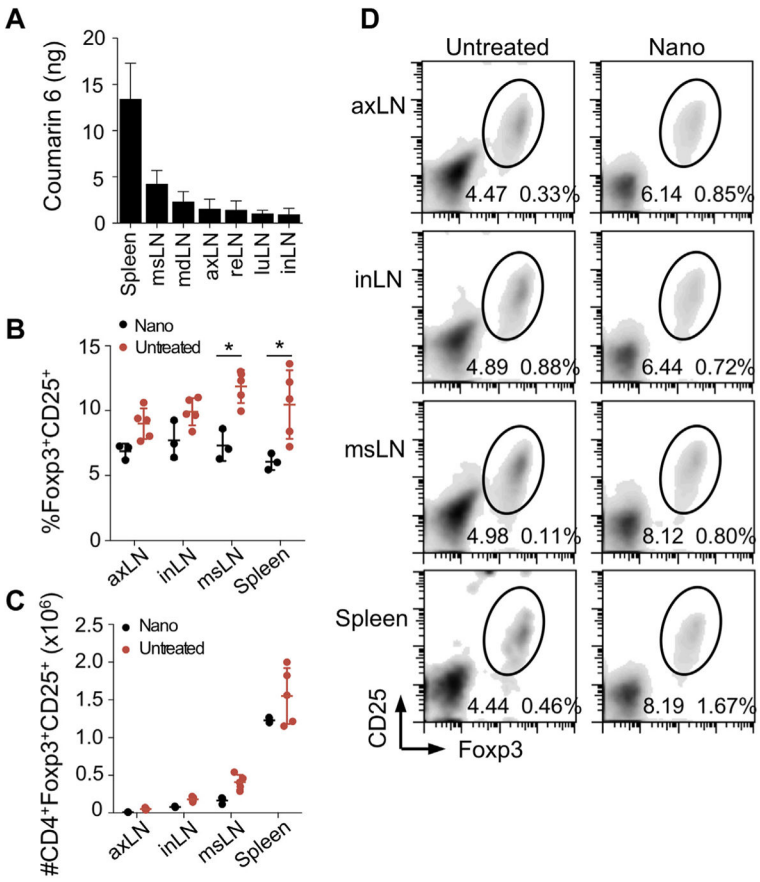

Fig. 6.

Nanoparticles enhance Tregs *in-vivo*. (A) 2.0 mg coumarin-6 labeled nanoparticles were injected I.P. and tissues were harvested after 5 days. Coumarin-6 was measured by fluorescence microscopy. (B–D) 2.0 mg TGF-β IL-2 CD4-targeted nanoparticles were injected I.P. and mice were sacrificed after 5 days for FACS analysis. (B) Tregs are plotted as percentages of $CD4^+$ T cells (*$p < 0.05$ vs. untreated controls). (C) Treg numbers per tissue are plotted. (D) Representative FACS plots are gated on $CD4^+$ lymphocytes. Values on the lower left of the gate show Tregs as a percentage of $CD4^+$ cells. Values to the right show Tregs as a percentage of all lymphocytes.

Table 1

Definitions of Fig. 4 notation.

Notation

A_y^x where: A is either the frequency f in terms of percentage, or number N of cells per sample well

x is the parent population from which A is gated

y describes the given population

For Example:

$N_{1.1+}^{CD4}$ = Number of Cells (N) per sample from a Thy1.1+ cell population that are CD4$^+$.

or;

$f_{1.1+}^{CD4}$ = Percent frequency (f) per sample from a Thy1.1$^+$ cell population that are CD4$^+$.

Notation	Definition
$N_{1.1+}^{CD4}$	Final number (per well) of responder cells (Thy1.1$^+$)
$N_{1.1+,\ i}^{CD4}$	Initial number (per well) of responder cells (Thy1.1$^+$)
$N_{1.1-}^{CD4}$	Final number (per well) of suppressor cells (Thy1.1$^+$)
$f_{1.1+}^{CD4}$	Final frequency (%) of responder cells (Thy1.1$^+$) from all CD4
$f_{1.1+,\ i}^{CD4}$	Initial frequency (%) of responder cells (Thy1.1$^+$) from all CD4
$f_{1.1-}^{CD4}$	Final frequency (%) of suppressor cells (Thy1.1$^-$) from all CD4
$f_{1.1-Foxp3+,\ i}^{CD4}$	Initial frequency (%) of Foxp3$^+$ suppressor cells (Thy1.1$^-$) from all CD4
$f_{Foxp3+}^{1.1-}$	Final frequency (%) of Foxp3$^+$ cells from suppressor (Thy1.1$^-$) population
$N_{Foxp3+}^{1.1-}$	Final number (per well) of Foxp3$^+$ cells from suppressor (Thy1.1$^-$) population
$N_{Foxp3+,\ i}^{1.1-}$	Initial number (per well) of Foxp3$^+$ cells from suppressor (Thy1.1$^-$) population

Table 2

Definitions of Fig. 4 characterization terms.

Term	Definition
Proliferative index, PI	$= \sum_0^g f_g^{1.1+} / \sum_0^g (f_g^{1.1+}/2^g)^a$
Initial Treg fraction[b]	$= f^{CD4}_{1.1-Foxp3+,\ i} / (f^{CD4}_{1.1-Foxp3+,\ i} + f^{CD4}_{1.1+,\ i})$
Final Treg number (per well), $N^{1.1-}_{Foxp3+}$	$= (PI) \times (f^{CD4}_{1.1-}/100) \times (f^{1.1-}_{Foxp3+}/100) \times 10^5$[c]

[a] Where g is generation number (0 is undivided population) and f_g is frequency of events in generation g.

[b] "Initial" refers to the start of the suppression phase (day 5).

[c] $N^{1.1-}_{Foxp3+,\ i} + N^{CD4}_{1.1+,\ i} = 10^5$.